Adsorption (2011) 17: 561–571
DOI 10.1007/s10450-011-9327-5

# Characterization of Supported Ionic Liquid Phase (SILP) materials prepared from different supports

**Jesus Lemus · Jose Palomar · Miguel A. Gilarranz · Juan J. Rodriguez**

Received: 15 August 2010 / Accepted: 18 January 2011 / Published online: 1 February 2011


**Abstract** Supported ionic liquid phase (SILP) materials are a recent concept where a film of ionic liquid (IL) is immobilized on a solid phase, combining the advantages of ILs (non volatility, high solvent capacity, etc.) with those of heterogeneous support materials. In this work, new SILP materials were prepared using a series of supports with different porosity and chemical nature. An imidazolium-based IL, 1-methyl-3-octylimidazolium hexafluorophosphate (OmimPF$_6$), was confined at variable contents (5–60% w/w) in three different activated carbons (ACs), silica (SiO$_2$), alumina (Al$_2$O$_3$) and titania (TiO$_2$).

For the first time, a systematic characterization of different SILP systems has been carried out applying a variety of analytical and spectroscopic techniques to provide information of interest on these materials. Elemental analysis (EA), adsorption–desorption isotherms of N$_2$ at 77 K, mercury porosimetry, termogravimetric analysis (TGA), differential scanning calorimetry (DSC), scanning electronic microscopy (SEM) and energy dispersive X-ray (EDX) were conducted to explore confinement effects. The results demonstrate that EA is a useful tool for quantifying the amount of imidazolium-based IL incorporated on support, independently of the nature of the solid. An excellent correlation has been obtained between the percentage of elemental nitrogen and the IL loaded on the support. The combination of nitrogen adsorption–desorption isotherms at 77 K and mercury porosimetry measurements was used to characterize the pore structure of both supports and SILP materials. It was found that depending on the available pores in the solid support, the IL tends to fill micropores firstly, then mesopores and lately in macropores. Thermal properties of SILP materials were studied herein by using both TGA and DSC methods, evidencing that the stability of SILP materials and the decomposition mechanism are strongly dependent on the surface chemistry of the solid support. SEM and EDX provided evidences of external surface coverage by ILs and filling of macropores at high IL load.

**Keywords** Ionic liquids · SILP · Supported ionic liquid phase · Characterization · Activated carbon · Porous structure · Thermal stability

## 1 Introduction

ILs posses an array of properties that make them attractive for academy and industry: extremely low vapor pressure, high thermal and chemical stabilities, non-flammability and high solvent capacity (Welton 1999; Wasserscheid and Welton 2008; Rogers and Seddon 2003). Moreover, the solvent properties of the IL are tunable by the choice of the cation/anion combination (Riisager et al. 2003). Because of their unique properties the applications of ILs have been expanding in various fields (Rogers and Seddon 2005). Thus, ILs have been extensively examined as an alternative to conventional organic solvents in reaction and separation processes (Rogers and Seddon 2005; Han and Armstrong 2007). There are a number of advantages of ILs in separation and reaction systems, but in many cases there is a need to immobilize them on porous materials (Wasserscheid and Welton 2008). The supported ILs can be spread on the inner surface of the porous structure, maintaining large specific surface area and mechanical properties of the support, thus circumventing the problem of mass transport limitation and the need for high amounts of ILs (Zhang et al. 2009a;

J. Lemus · J. Palomar · M.A. Gilarranz · J.J. Rodriguez (✉)
Seccion de Ingenieria Quimica, Universidad Autonoma de Madrid, Cantoblanco, 28049 Madrid, Spain
e-mail: juanjo.rodriguez@uam.es

Vangeli et al. 2010). The resulting material is usually referred as supported ionic liquid phase (SILP).

The SILP concept results in a very efficient use of the IL, because of relatively short diffusion distances for the reactants compared to those in conventional two-phase systems with an IL phase. In addition, the negligible vapor pressure, large liquid range, and thermal stability of ILs ensure that the solvent is retained on the support in its fluid state even at elevated temperatures; this makes SILP highly suitable for continuous processes.

The latest developments in SILP systems can be divided in two great blocks as catalysis (Riisager et al. 2003, 2005b, 2006a, 2006b; Virtanen et al. 2007, 2009a, 2009b; Ruta et al. 2008) and separation processes (Zhang et al. 2009a; Vioux et al. 2010; Sun et al. 2009; Fontanals et al. 2009; Fang et al. 2010; Kohler et al. 2010; Werner et al. 2010; Joni et al. 2010). In catalytic processes, a variety of reactions have been studied where SILP proved to be more active and selective than common systems. The final role that can be played by an IL in a catalytic process is simply as the solvent for the reaction and in this role SILP have been most widely used. Most studies in this topic have been focused on the screening of type reactions and the development of new SILP materials for hydroformylations, hydrogenations, and C–C coupling reactions, among others, is being widely investigated. The combination of well-defined catalyst complexes, non-volatile ILs, and porous solid supports offers many advantages over traditional catalysis in aqueous phase or conventional organic solvents, which are clearly limited by the volatility of the solvent. The SILP concept is considered as a significant contribution to the development of highly selective heterogeneized homogeneous catalysts (Riisager et al. 2005a). The use of SILP in separation applications has also awakened interest as alternative to traditional separation and purification processes of $SO_2$ as hydrodesulfuration (Zhang et al. 2009a; Kohler et al. 2010). $SO_2$ can be absorbed in SILP materials with a high absorption capacity and selectivity (Wu et al. 2004) and numerous ILs with $SO_2$ sorption ability have been reported (Huang et al. 2006). Likewise, $CO_2$ separation and purification processes have also been extensively reported (Ilconich et al. 2007; Bara et al. 2009), based on the high solubility values of $CO_2$ in some ILs. SILP materials were prepared from a broad range of imidazolium-based ILs at loads varying from 5 to 60% (w/w) (Zhang et al. 2009a; Kohler et al. 2010; Ilconich et al. 2007; Bara et al. 2009).

Because of the great advantages of SILP materials and the need of a deeper understanding of their properties as reaction and separation media, the aim of this work was to gather characterization methods for SILP materials, including elemental analysis, chemical composition, porous structure, thermal stability and morphology.

Immobilization of ILs as thin layers on porous materials can be achieved simply by physisorption or by chemical binding to the support of one of the ions that compose the IL (Virtanen et al. 2009a). In this work, six solids of different porosity and chemical nature have been studied as supports for SILP materials. They can be grouped into three classes based on their pore diameter: microporous, $d <$ 2.0 nm; mesoporous, $2.0 < d < 50$ nm; and macroporous, $d > 50$ nm (Zhang et al. 2009b). A diversity of support materials were selected of different chemical nature among those commonly used in SILP preparation, like $TiO_2$ (Chen et al. 2007), $SiO_2$ (Zhang et al. 2009a; Vangeli et al. 2010; Fang et al. 2010; Mehnert 2005) or AC (Virtanen et al. 2009a; Kohler et al. 2010) among others (Riisager et al. 2006b). In an earlier work, Palomar et al. (2009) showed the possibility of following the amount of imidazolium-based IL on AC supports by measuring the percentage of elemental nitrogen in SILP from EA and it has been herein extended to several supports and SILP systems in order to generalize the use of this technique for direct quantification of IL loaded on SILP materials. Structural properties of highly porous supports and SILP materials were analyzed, using adsorption–desorption isotherms of $N_2$ at 77 K and mercury porosimetry. Both techniques give information on the available volume of micro, meso and macropores available and have been used in previous works showing the difference between a fresh support and a SILP material (Vangeli et al. 2010; Zhang et al. 2009b; Chen et al. 2007; Shi and Deng 2005). Thus, a systematic study on the variation of the porous structure has been carried out with the aim of better understanding how the IL is distributed onto the supports. In addition, results on the thermal stability of SILP materials at high temperature by means of TGA and DSC analysis are collected herein together for the first time. To the best of our knowledge, only thermal studies of ILs have been so far reported (Fernandez et al. 2007; Holbrey et al. 2002; Karna et al. 2009), but without analyzing the relationship between IL and support, except two recent works where a thermal study of SILP materials has been reported (Vangeli et al. 2010; Kohler et al. 2010). Some of the works published in the literature (Zhang et al. 2009a; Vangeli et al. 2010; Kohler et al. 2010; Muldoon 2010; Kim et al. 2002) showed SILP applications at high temperatures based on different supports. In the present work, a representative collection of supports has been investigated. Finally, the morphology and chemical composition of the surface of SILP materials have been analyzed via SEM-EDX. To the best of our knowledge, a work gathering these techniques for characterization of SILP materials has not been so far reported.

## 2 Experimental methods

### 2.1 Materials and reagents

All chemicals used in the experiments were analytical grade and were used without further purifications. $OmimPF_6$ was supplied by Iolitec in the highest purity available (purity >99%). The adsorbents used in this study were the following: CAPSUPER supplied by Norit, MkU supplied by Merck, ENA250G supplied by Timcal, $SiO_2$, $Al_2O_3$ and $TiO_2$ supplied by Sigma-Aldrich. Acetone (purity >99.5%) used in SILP preparation was supplied by Panreac.

To immobilize an IL the selection of support type and immobilization method are important depending on its application (Zhang et al. 2009a). Immobilization or supporting of ILs can be carried out in many different ways, such as simple impregnation, grafting, polymerization sol-gel method, encapsulation or pore trapping, among others (Virtanen et al. 2009a). In this work, a straightforward preparation method of SILP materials based on a direct impregnation of the support material with $OmimPF_6$, dissolved in acetone was applied. To prevent hydration, IL and acetone were kept in their original tightly closed bottles in a desiccator before use. When any chemicals were used, they were always manipulated inside a glovebox under a dry nitrogen atmosphere. Impregnation was carried out mixing 1 ml of $OmimPF_6$ dissolved in acetone for each 100 mg of support. $OmimPF_6$ concentration in acetone solution was adjusted to obtain different IL loadings on the support. To ensure a homogeneous penetration of the IL solution into the pores, stirring in an orbital shaker for 1.5 h was applied followed by vacuum evacuation of acetone at 10 mbar and 333 K over 2 h. Then, SILP materials were stored at 333 K during 24 h prior to their characterization. After vacuum evaporation of acetone, the SILP contains from 5 to 60% (w/w) of IL phase. To check the amount of IL immobilized on the supporting material, all the supports and SILP materials were weighed before and after impregnation. The mass percentages given in this work for IL load are SILP basis. All the SILP materials prepared had the resemblance and behavior of a powdered material. As a first approach, different commercially available supports with a variety of porosities and chemical natures were used to incorporate IL in their pore structure. Three activated carbons (CAPSUPER, MkU and ENA250G), $SiO_2$, $Al_2O_3$ and $TiO_2$ were used to evaluate the influence of the chemical surface. Table 1 summarizes the supporting characteristics of the supports.

### 2.2 Characterization and instruments

The chemical nature of the supports and SILP materials was determined by means of EA in a Perkin–Elmer analyzer (LECO CHNS-932 model) to obtain C, H and N percentages. Volatile matter was calculated by difference between the weight of fresh support and after ten minutes in a ceramic vessel at 900 °C under nitrogen atmosphere. Ash matter was calculated by difference between the weight of fresh support and after eight hours in a ceramic vessel at 650 °C under oxidizing atmosphere. The $pH_{slurry}$ was determined measuring, until constant value, the pH of an aqueous suspension of support in distilled water (1 g/10 ml).

The porous structure of supports and SILP materials was characterized by means of nitrogen adsorption–desorption isotherms at 77 K using a Micromeritics apparatus (Tristar II 3020 model) and mercury porosimetry using Quantachrome apparatus (PM-3310 model). Before adsorption–desorption experiments, samples were outgassed at 150 °C under a residual pressure lower than $10^{-3}$ Pa. The BET equation was applied to determine the BET surface area ($A_{BET}$) and Dubinin–Radushkevich equation for micropore volume. The external area ($A_s$) was obtained from the t-method. The difference between $N_2$ adsorbed volume at 0.95 of relative pressure and the micropore volume was taken as mesopore volume. In the mercury porosimetry measurements the estimation of pore diameter from the applied pressure was based on the Washburn equation. The surface tension of mercury was taken as $4.8 \times 10^{-3}$ N/cm and the mercury contact angle as 141°.

Thermogravimetric analysis (TGA) of $OmimPF_6$, supports and SILP materials was conducted on a Mettler Toledo Instrument (TGA/SDTA851e model) under nitrogen with a heating rat of 10 °C/min. The accuracy of temperature and mass measurements was 0.1 °C and $10^{-3}$ mg, respectively. A dynamic method was used with a temperature range from 50 to 600 °C at a heating rate of 10 °C $min^{-1}$ while purging with 50 ml $min^{-1}$ of dry nitrogen. The mass of the sample placed in TGA analyses were between 4 and 12 mg. In all TGA runs, aluminum pans with a capacity of 70 ml were used.

Differential scanning calorimetry (DSC) analyses of $OmimPF_6$, solid supports and SILP materials were carried out on a Mettler Toledo instrument (DSC/821e model). The temperature measurements were carried out with accuracy better than 0.1 °C. DSC curves of samples were determined at a 10 °C $min^{-1}$ heating rate between 50 and 600 °C. In all experiments, stainless steel pans with a volume of 120 µl and a purge flow of 50 ml $min^{-1}$ of dry nitrogen were used. The sample mass range used in DSC experiments was between 10 and 20 mg.

The morphology of the IL layer on the carbonaceous support was characterized by scanning electron microscopy (SEM) (Hitachi S-3000N model) before and after IL phase deposition. The samples were placed in the microscope chamber after gold metallization treatment; SEM micrographs at 25000× were taken with an accelerating voltage of 20 kV. SEM was equipped with an energy dispersive X-ray (EDX) analyzer (INCAx-sight model). EDX was used to

**Table 1** Characterization of the supports

| Nomenclature | Source | $A_{BET}$ | $A_s$ | $V_{microp.}$ | $V_{mesop.}$ | $V_{macrop.}$ | $V_{Total}$ | %C | %H | %N | %Volatile | %Ash | $pH_{slurry}$ |
|---|---|---|---|---|---|---|---|---|---|---|---|---|---|
| CAPSUPER | NORIT | 1915 | 667 | 0.66 | 0.63 | 1.02 | 2.32 | 81.0 | 2.30 | 0.43 | 14.0 | 1.80 | 3.3 |
| MkU | MERCK | 927 | 155 | 0.36 | 0.14 | 0.22 | 0.72 | 88.9 | 0.66 | 0.57 | 3.49 | 5.30 | 5.4 |
| ENA250G | TIMCAL | 79 | 68 | 0.00 | 0.08 | 1.40 | 1.48 | 98.8 | 0.17 | 0.03 | 2.40 | 0.00 | 6.1 |
| $TiO_2$ | SIGMA | 50 | 45 | 0.00 | 0.06 | 0.96 | 1.02 | 0.23 | 0.16 | 0.05 | 1.05 | 98.9 | 5.6 |
| $SiO_2$ | SIGMA | 212 | 212 | 0.00 | 0.26 | 3.07 | 3.32 | 0.23 | 1.95 | 0.03 | 0.10 | 98.7 | 6.7 |
| $Al_2O_3$ | SIGMA | 136 | 136 | 0.00 | 0.21 | 0.12 | 0.33 | 0.10 | 0.74 | 0.02 | 5.88 | 98.4 | 8.1 |
| | | $A$ ($m^2\ g^{-1}$); $V_{pore}$ ($cm^3\ g^{-1}$) | | | | | | | | | | | |

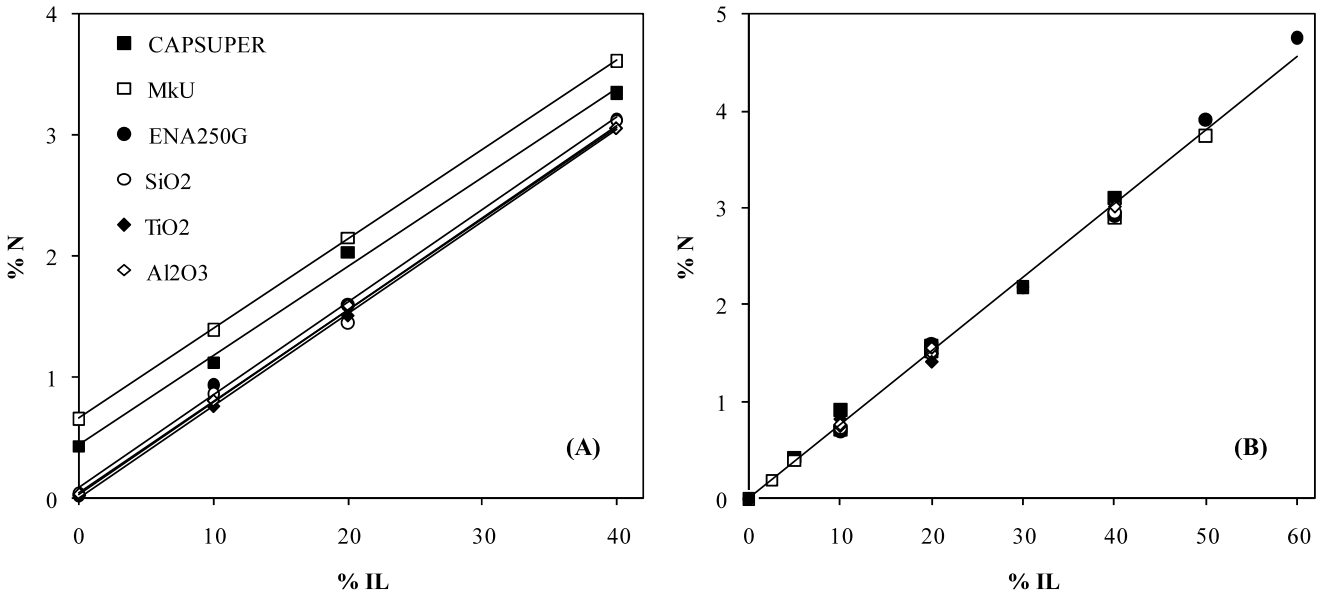


**Fig. 1** Mass percentage of elemental nitrogen of SILP materials against the $OmimPF_6$ load (**a**) total nitrogen and (**b**) normalized nitrogen excluding nitrogen from the support

study the distribution of the different chemical elements of interest in the supported IL.

## 3 Results and discussion

### 3.1 Quantification of the IL amount on SILP materials

The development of quantitative procedures for determining the amount of IL incorporated to the supports is of interest not only to check SILP materials preparation, but also to evaluate the stability in applications where IL losses can occur. In a previous work (Palomar et al. 2009), a method based on EA was proposed as a procedure to determine the load of $OmimPF_6$ on AC, thus a linear regression was found between the percentage of elemental nitrogen obtained by EA and the weight percentage of IL incorporated on the support. In this work, the analytical process is extended to six different supports, as depicted in Fig. 1a, where the same linear dependence was found for all the SILP material supports. As can be seen, the $y$-intercept of the lineal correlations of Fig. 1a depends on the initial amount of nitrogen in the starting support (see Table 1). Normalized nitrogen contents were calculated excluding the nitrogen content of the starting support from SILP material. A very good correlation was obtained, as shown in Fig. 1b. Therefore, EA can be considered as a quantitative tool for determining the amount of IL supported on SILP materials and it has been used to calculate with accuracy the contribution of IL to SILP materials in this work.

### 3.2 Textural properties of SILP materials

ILs in SILP materials may be distributed on both the external and internal surface of the supports. Adsorption–desorption isotherms of $N_2$ at 77 K have been previously used to obtain information about the effect of ILs on the available micro and mesopores of the supports (Zhang et al. 2009a, 2009b).

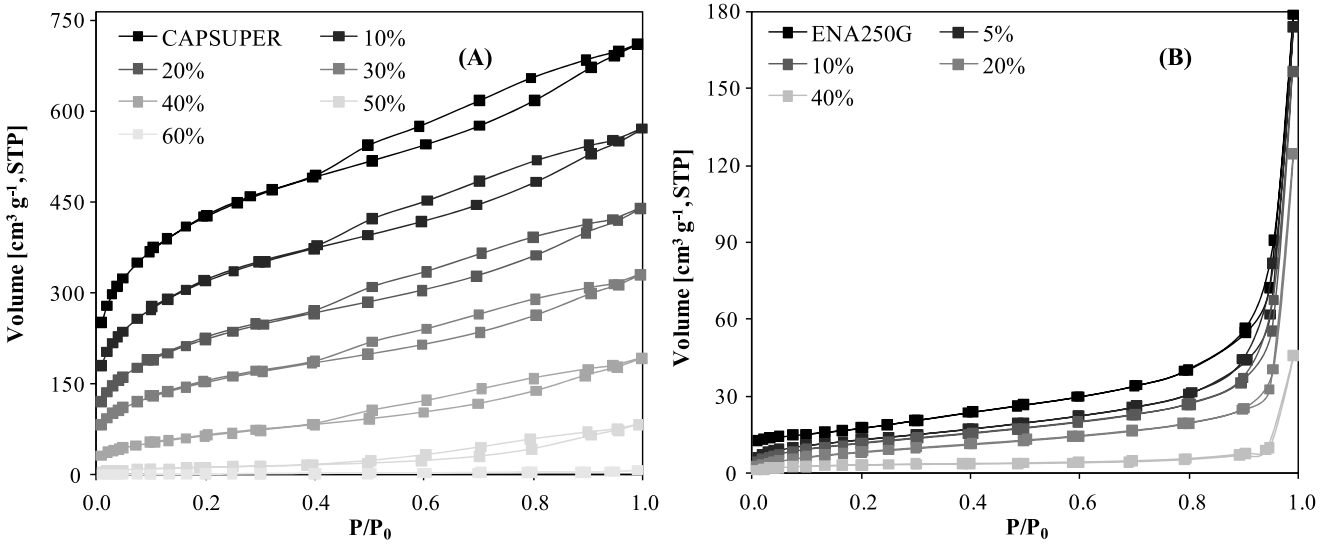


**Fig. 2** Nitrogen adsorption–desorption isotherms at 77 K of SILP with increasing amounts of $OmimPF_6$ (0–60% w/w) on CAPSUPER (**a**) and ENA250G (**b**)

Figure 2 shows the adsorption–desorption isotherms obtained for two ACs of fairly different porous structure (CAPSUPER and ENA250G) at increasing loads of IL from 0 to 60% (w/w). The incorporation of IL to CAPSUPER structure leads to preferential loss of micropore volume, probably by filling or blocking of that pore range by IL. The hysteresis and the slope of the adsorption–desorption isotherms show that the loss of mesopore volume becomes significant for IL contents above 20%, suggesting a hierarchical mechanism of pore filling during impregnation with IL. For an IL load of 50% the SILP material does not show a significant microporosity but maintains some mesoporosity, which disappears when the IL load is increased to 60%. In the case of the SILP materials prepared from ENA250G, a maximum IL load of 40% was achieved in order to maintain powdered texture and avoid agglomeration. The series of SILP materials from ENA250G showed a progressive loss of porosity in the whole range of pore size during impregnation, as can be inferred from the isotherms. Although CAPSUPER and ENA250G differ substantially in porosity, the maximum load of IL incorporated is comparable. This result shows the important role that macroporosity can play in the retention of ILs.

In order to generalize the observation commented for Fig. 2, the BET surface area of four SILP materials with increasing loads of $OmimPF_6$ were plotted in Fig. 3, where it can be appreciated that supports of different porosity present BET surface affected on various ways. Thus, microporous supports (CAPSUPER and MkU) lose surface area in a larger extent with the incorporation of IL, while mesoporous and macroporous materials undergo a lower loss of surface area although they are capable of retaining similar IL loads.

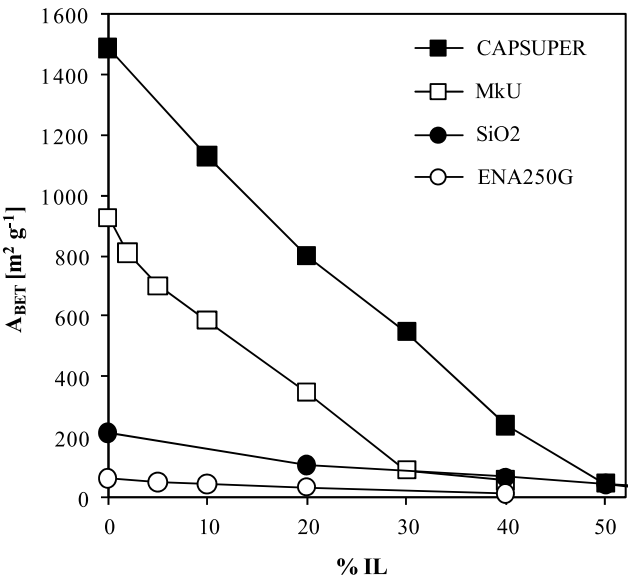


**Fig. 3** Variation of BET surface area of CAPSUPER, MkU, $SiO_2$ and ENA250G at increasing $OmimPF_6$ loads (0–50% w/w)

In order to evaluate the distribution of IL onto the mesoporous and macroporous structure, mercury porosimetry of supports and SILP materials was carried out. Figure 4 shows the pore size distribution against pore diameter of SILP materials prepared with two kinds of supports for different IL loads. CAPSUPER support has a high contribution of mesopore volume that is lost progressively with increasing IL load. According to the nitrogen adsorption–desorption isotherms, some mesoporosity remains up to loads of 40–50%, and almost complete loss of mesoporosity takes place at 60% IL load. On the other hand, ENA250G shows a significant contribution of pores with diameter cen-

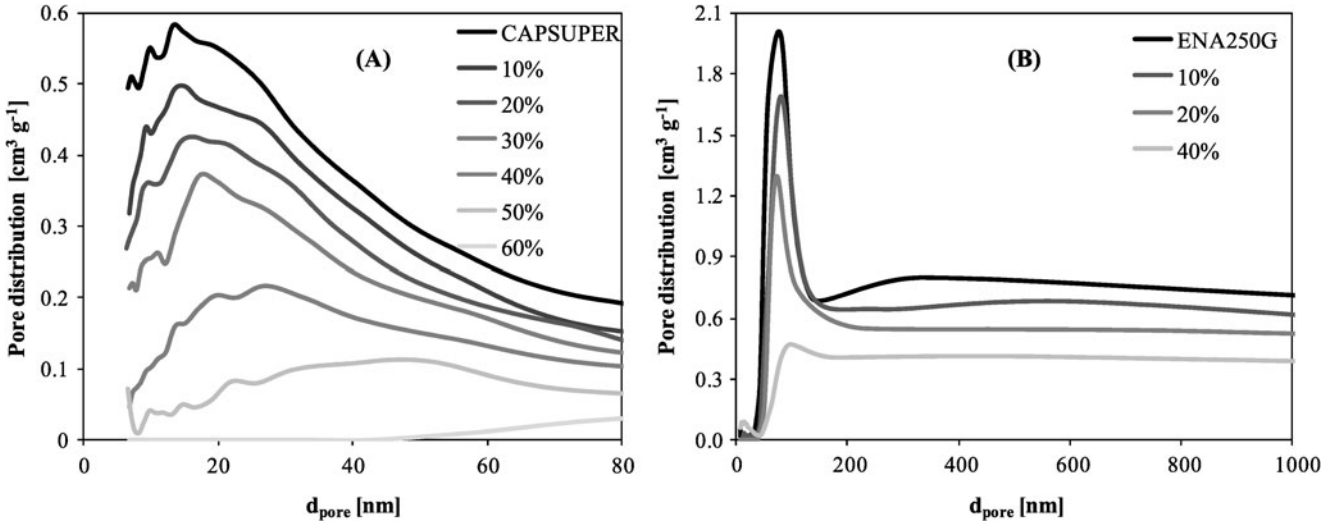


**Fig. 4** Pore size distribution (6 to 1000 nm) at increasing amounts of $OmimPF_6$ (from 0 to 60% (w/w)) on (**a**) CAPSUPER and (**b**) ENA250G as obtained from mercury porosimetry

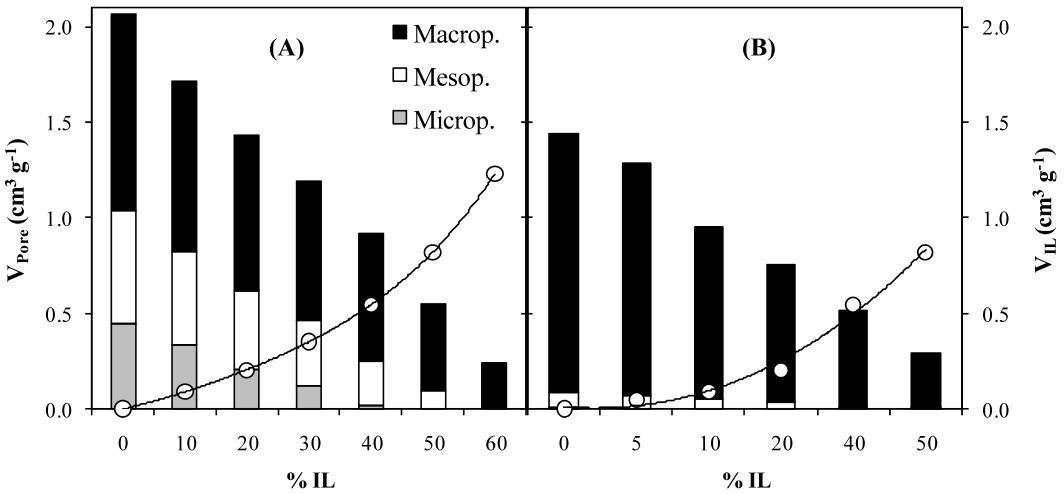


**Fig. 5** Pore size distribution at increasing amounts of $OmimPF_6$ (from 0 to 50–60%) on (**a**) CAPSUPER and (**b**) ENA250G as obtained from the combination of adsorption–desorpiton isotherms of $N_2$ at 77 K and mercury porosimetry and estimated volume occupied by the loaded IL (○)

tered around 100 nm that are gradually filled as the amount of IL is increased, together with a loss of porosity in the whole range of macropores. It must be remarked the difficulty of analyzing mercury porosimetry results for SILP materials, which contain both IL and a solid support, instead of simply a porous solid. However, for SILP characterization, both techniques nitrogen adsorption–desorption and mercury porosimetry were found highly complementary and can be grouped to obtain useful information about the distribution of ILs in SILP material, for comparison purposes between systems implying different IL loading and solid supports. The combination of both techniques provides the impregnation pattern shown for CAPSUPER and ENA250G in Fig. 5. In the case of CAPSUPER, IL seems to fill firstly the micropores followed then by mesopores and lately by macropores. On the contrary, in a support without micropore contribution such as ENA250G the filling takes place first in mesopores and afterward in macropores. As can be also seen in Fig. 5, there is a reasonable agreement between the amount of IL volume incorporated to the SILP material, calculated from the experimental molar density, and the gradual loss of the pore volume available in the support, which may suggest access of IL to a substantial proportion of the micropore volume.

The maximum IL load achieved in SILP materials against the total pore volume ($d_{pore} < 1000$ nm) quantified by combination of adsorption–desorption isotherms of $N_2$ at 77 K and mercury porosimetry is shown in Fig. 6. The excellent correlation makes possible to assume that supports with high pore volume are preferred if a large IL loading is in-

tended. Particularly interesting are the cases of CAPSUPER and $SiO_2$, which showed retention capacities of 63 and 77% (w/w), respectively, i.e. 1.7 and 3.3 grams of IL per gram of support. However, in certain cases lower IL loads may be desirable if maintaining some surface area of the SILP material is required for the specific application.

### 3.3 Thermal stability of SILP materials. TGA and DSC study

The thermal stability of SILP materials is of special interest for gas phase applications (Kohler et al. 2010; Wu et al. 2004; Huang et al. 2006), where high temperatures may be required. Even though the decomposition temperature of pure IL is above the process temperature, the interaction with the support may lead to reduced stability. As a first approach, the thermal stability of pure IL was examined by TGA and DSC within range of 50–600 °C. Previous works showed that common imidazolium-based ILs, such as $OmimPF_6$, have very high thermal decomposition temperature and that the anion decomposes before the cation (Fernandez et al. 2007). The TGA curve in Fig. 7 shows that $OmimPF_6$ started to decompose at 350 °C and it decomposed almost completely at 500 °C, without any char formation. Figure 7 reports DSC results for $OmimPF_6$ showing two exothermic peaks, which were assigned to $PF_6$ anion at 370 °C and subsequently imidazolium cation at 400 °C, consistently with previous TGA observations and the difference in molar mass of the counterions (Fernandez et al. 2007).

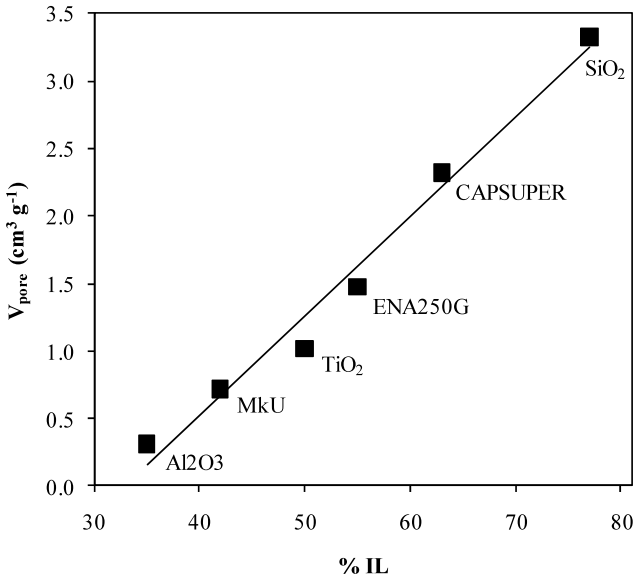


**Fig. 6** Total pore volume (up to 1000 nm) as obtained from the combination of adsorption–desorption isotherms of $N_2$ at 77 K and mercury porosimetry against maximum retention capacity of different supports at incipient wetness

Figure 8a shows the TGA curves of the supports after being subjected to oven drying at 105 °C for 2 hours. The mass losses of all the supports studied were below 6% at 600 °C. Figure 8b shows the DSC curves for six supports, where the lack of neat peaks confirms their high stability.

After separate evaluation of the thermal stability of IL and supports, the thermal stability of SILP materials was studied at IL loads of *ca.* 40% (w/w). Figure 9a depicts TGA and DTG for AC-based SILP materials. The stability is significantly influenced by the nature of the AC, being always lower than of pure IL. SILP material prepared using CAPSUPER support started to decompose at 200 °C, whereas those prepared with MkU started at 260 °C, however, the DTG peak, assigned to cation, is centered for both supports around 390 °C. The SILP based on ENA250G, showed higher thermal stability, starting to decompose at 360 °C and presenting the DTG peak of cation at 450 °C. DSC plots also

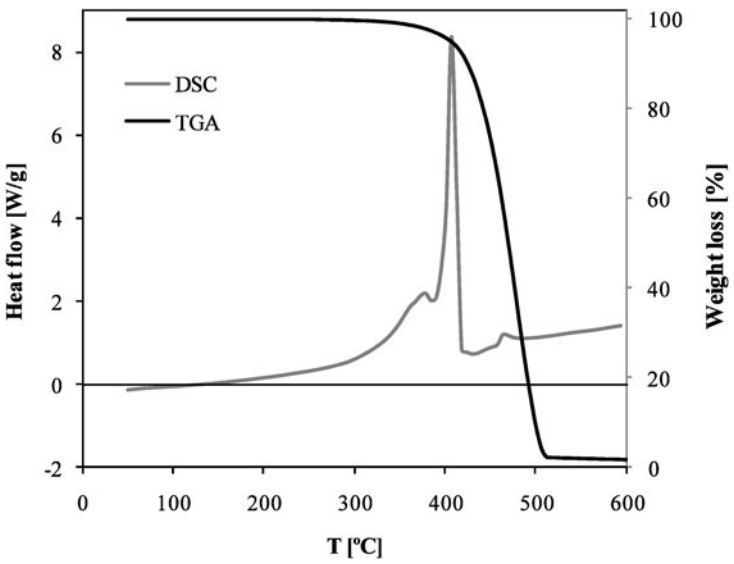


**Fig. 7** TGA (*black line*) and DSC (*gray line*) curves of $OmimPF_6$ under nitrogen atmosphere with a heating rate of 10 °C/min

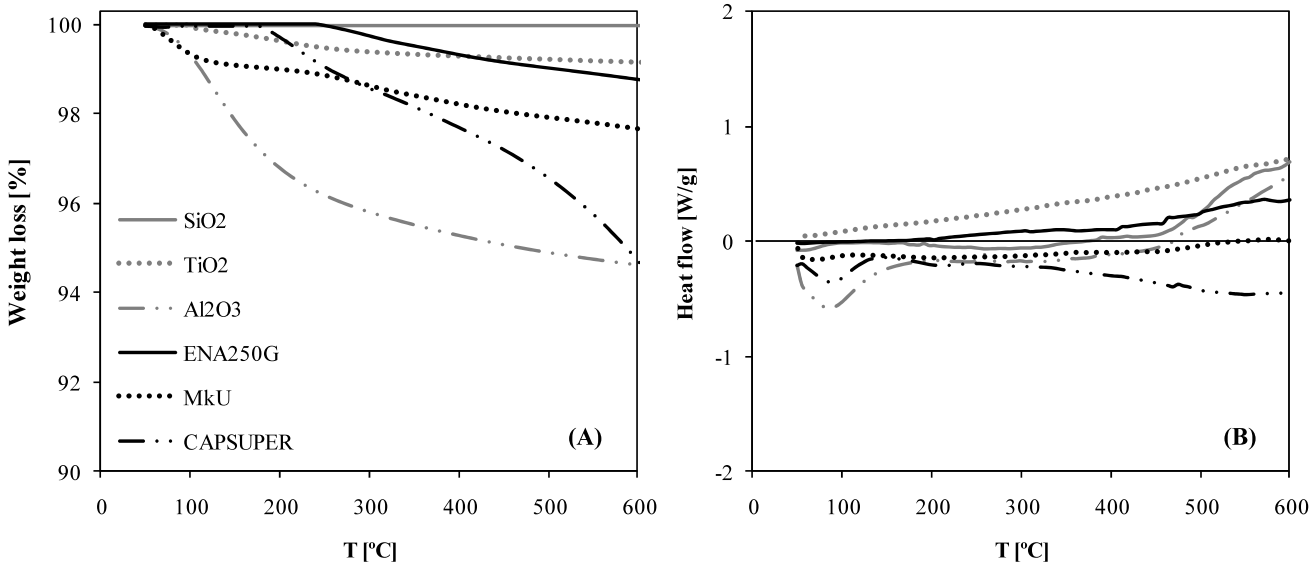


**Fig. 8** TGA (**a**) and DSC (**b**) curves of the supports under nitrogen atmosphere at a heating rate of 10 °C/min

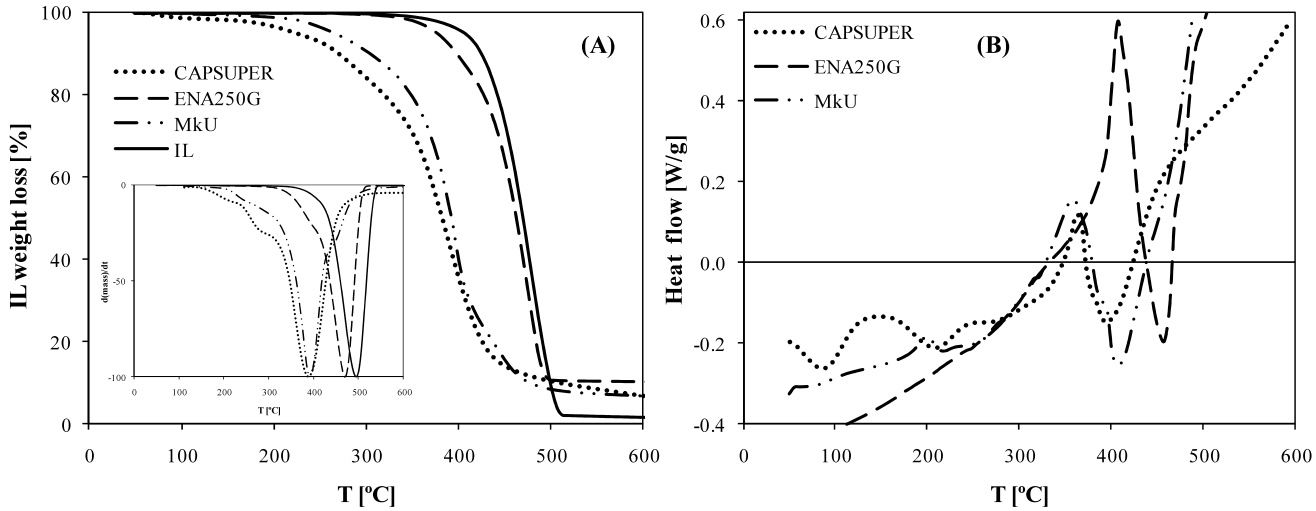


**Fig. 9** (**a**) TGA curves and DGT peaks obtained under nitrogen at a heating rate of 10 °C $min^{-1}$ for $OmimPF_6$ and SILP materials based on ACs loaded at *ca*. 40 wt % and (**b**) the corresponding DSC curves for SILP materials

show the changes in the thermal stability of IL due to the influence of the support (Fig. 9b). In fact, DSC peaks coincide with the peak minima from TGA derivation, showing the agreement between both techniques. Moreover, whereas both decomposition peaks of DSC (anion and cation) are exothermic for pure IL, SILP materials present an exothermic peak assigned to anion and, subsequently, an endothermic peak allocated to cation that is endothermic. Attending to Table 1, the chemical nature of supports surface plays a main role in the thermal stability of SILP material. Measurements of $pH_{slurry}$ of carbonaceous supports indicate that the acidity of the support increases in the order ENA250 < MKU < CAPSUPER, i.e., the same order observed for decreasing anion decomposition temperature by TGA and DSC. The higher acidity of CAPSUPER and MkU, together with their higher surface area, seems to promote cracking of anion thus lowering the thermal decomposition temperature. The role of acid sites in promoting thermal decomposition reactions is a well known fact for cracking catalysts (van Grieken et al. 2001). As indicated above, the thermal decomposition of cation was described by an endothermic process, which suggests a different decomposition mechanism. This hypothesis is supported by the formation of pyrolityc carbon from the decomposition of the organic part of IL (imidazolium cation), which was not observed for pure IL (see Fig. 9a).

In the cases of SILP materials not supported on AC, a remarkable effect of the nature of the support on SILP thermal

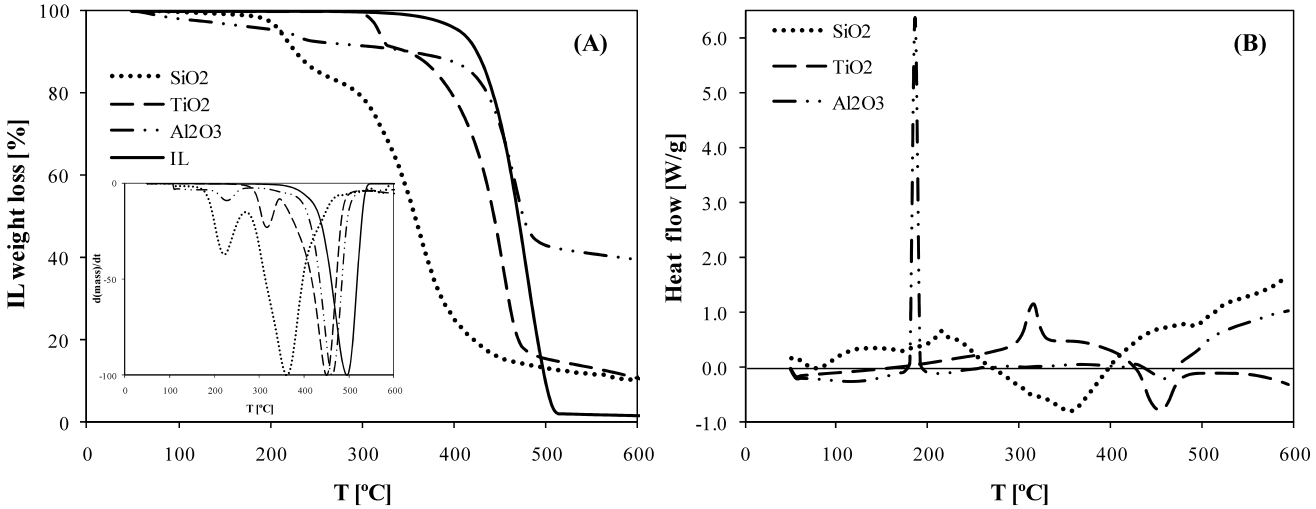


**Fig. 10** (**a**) TGA curves and DGT peaks obtained under nitrogen at a heating rate of 10 °C min$^{-1}$ for $OmimPF_6$ and SILP materials not supported on AC loaded at *ca*. 40 wt % and (**b**) the corresponding DSC curves for SILP materials

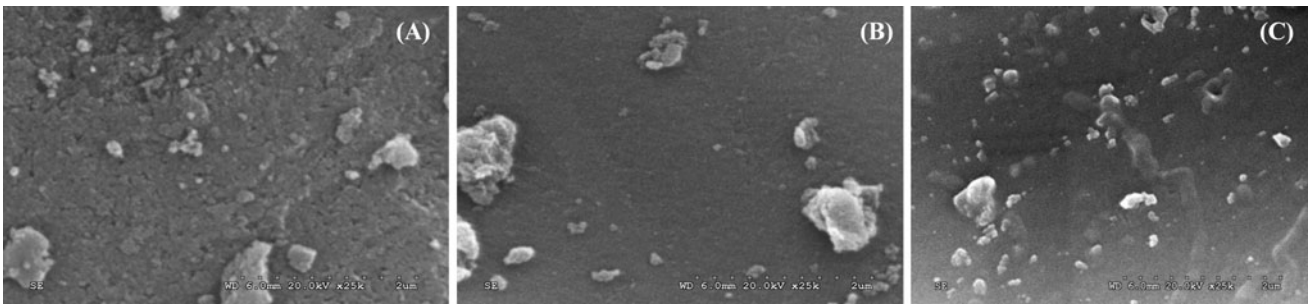


**Fig. 11** SEM images (×25000) of CAPSUPER support (**a**) and SILP with an IL load of 40% (**b**) and 60% (w/w) (**c**)

**Table 2** Temperatures (K) of DTG and DSC peaks curves assigned to cation and anion of OmimPFe in the solid supports

| | $T_{cation\text{-}DTG}$ | $T_{cation\text{-}DSC}$ | $T_{Anion\text{-}DTG}$ | $T_{Anion\text{-}DSC}$ |
|---|---|---|---|---|
| CAPSUPER | 390 | 396 | 280 | 362 |
| MkU | 393 | 401 | 290 | 350 |
| ENA250G | 450 | 452 | 383 | 407 |
| $A1_2O_3$ | 463 | 458 | 220 | 198 |
| $TiO_2$ | 450 | 447 | 315 | 303 |
| $SiO_2$ | 360 | 350 | 220 | 209 |

**Table 3** Percentages of C, O, F and P from EDX of CAPSUPER and SILP loaded at 40 and 60% (w/w)

| | CAPSUPER | SILP 40% | SILP 60% |
|---|---|---|---|
| %C | 85.9 | 77.5 | 77.8 |
| %O | 13.8 | 12.8 | 11.2 |
| %F | 0.00 | 7.70 | 8.68 |
| %P | 0.31 | 2.07 | 2.35 |

stability can also be observed. The mass loss allocated to anion and cation appears at different temperatures depending on the supporting material (see Fig. 10a). Silica is the most polar support and decomposition occurs before than for the rest (195 °C). $Al_2O_3$-based SILP decomposed at 215 °C, although overlapped with the weight loss of the own $Al_2O_3$ support. Lately, $TiO_2$ decomposed clearly at 310 °C. Figure 10b shows DSC curves for SILP materials supported on $SiO_2$, $Al_2O_3$ and $TiO_2$, presenting an exothermic peak assigned to anion and subsequently an endothermic peak assigned to cation. Table 2 summarizes the temperatures for DTG and DSC peaks for the six SILP materials prepared. The DSC peaks are in agreement with the DTG ones, showing the consistency of both techniques for the evaluation of thermal stability. Further studies of thermal stability of SILP supported on organic and inorganic materials must be developed in the future to provide insight into the role of the surface chemistry of the supports, being TGA and DSC useful tools.

### 3.4 SEM and EDX studies

Scanning electron microscopy (SEM) combined with energy dispersive X-rays (EDX) analysis were used to examine the CAPSUPER AC surface and obtain information about its chemical composition before and after impregnation with IL. Figure 11 shows a progressive smoothing of the SILP surface with increasing IL load, particularly for a load of 60%, which indicates filling of macropores and some excess of IL on the surface. Table 3 provides results on the average chemical composition of the support and SILP materials surface, indicating a similar composition for the SILP materials with 40 and 60% IL load. The fluorine signal corresponding to the $PF_6$ cation indicates uniform distribution of IL on the external surface of the support for a 40% load, even though SEM does not indicate excess of IL filling macropores.

## 4 Conclusion

The concept of SILP has been examined for the sake of learning on future potential applications in the fields of catalytic and separation processes. Using supports of different porous structures and ILs of different properties (polar nature) SILP systems can be designed and prepared for specific applications. In this work, we evaluated and proposed different techniques to characterize SILP materials, which may be applied in the future to relate their properties and behavior as reaction or separation media. Thus, EA has been demonstrated as a useful analytical tool to accurately quantify the amount of imidazolium-based IL loaded onto the support, through the percentage of elemental nitrogen. On the other hand, adsorption–desorption isotherm of $N_2$ at 77 K and mercury porosimetry have been successfully used to describe the distribution of IL onto the support surface for a variety of SILP materials. Attending to support porosity it was found that IL fills selectively small pores, but, when they do not exit, IL is charged on the available pores, as it happens with macroporous $SiO_2$. The amount of IL can be modulated depending on the application of SILP, but when a SILP material with a high IL load is required a highly porous support is needed. These SILP materials have a high IL content but they lose their pore structure. Finally, TGA and DSC measurements were consistently applied to evaluate the thermal stability of the SILPs. It was found that the nature of the support can remarkably affect to the thermal stability of the SILP systems, resulting the most stable those SILP materials prepared from supports of non polar acidic character.

**Acknowledgements** The authors are grateful to the "Ministerio Ciencia e Innovación" and "Comunidad de Madrid" for financial support (CTQ2008-05641 and S2009/PPQ-1545).

## References

Bara, J.E., Carlisle, T.K., Gabriel, C.J., Camper, D., Finotello, A., Gin, D.L., et al.: Guide to $CO_2$ separations in imidazolium-based room-temperature ionic liquids. Ind. Eng. Chem. Res. **48**(6), 2739–2751 (2009)

Chen, S.Y., Han, C.C., Tsai, C.H., Huang, J., Chen-Yang, Y.W.: Effect of morphological properties of ionic liquid-templated mesoporous anatase $TiO_2$ on performance of PEMFC with Nafion/$TiO_2$ composite membrane at elevated temperature and low relative humidity. J. Power Sources **171**(2), 363–372 (2007)

Fang, G., Chen, J., Wang, J., He, J., Wang, S.: N-methylimidazolium ionic liquid-functionalized silica as a sorbent for selective solid-phase extraction of 12 sulfonylurea herbicides in environmental water and soil samples. J. Chromatogr. A **1217**(10), 1567–1574 (2010)

Fernandez, A., Torrecilla, J.S., Garcia, J., Rodriguez, F.: Thermophysical properties of 1-ethyl-3-methylimidazolium ethylsulfate and 1-butyl-3-methylimidazolium methylsulfate ionic liquids. J. Chem. Eng. Data **52**, 1979–1983 (2007)

Fontanals, N., Ronka, S., Borrull, F., Trochimczuk, A.W., Marcé, R.M.: Supported imidazolium ionic liquid phases: a new material for solid-phase extraction. Talanta **80**(1), 250–256 (2009)

Han, X., Armstrong, D.W.: Ionic liquids in separations. Acc. Chem. Res. **40**, 1079–1086 (2007)

Holbrey, J.D., Reichert, W.M., Swatloski, R.P., Broker, G.A., Pitner, W.R., Seddon, K.R., et al.: Efficient, halide free synthesis of new, low cost ionic liquids: 1,3-dialkylimidazolium salts containing methyl- and ethyl-sulfate anions. Green Chem. **4**(5), 407–413 (2002)

Huang, J., Riisager, A., Wasserscheid, P., Fehrmann, R.: Reversible physical absorption of $SO_2$ by ionic liquids. Chem. Commun. **38**, 4027–4029 (2006)

Ilconich, J., Myers, C., Pennline, H., Luebke, D.: Experimental investigation of the permeability and selectivity of supported ionic liquid membranes for $CO_2$/He separation at temperatures up to 125 °C. J. Membr. Sci. **298**(1–2), 41–47 (2007)

Joni, J., Haumann, M., Wasserscheid, P.: Continuous gas-phase isopropylation of toluene and cumene using highly acidic Supported Ionic Liquid Phase (SILP) catalysts. Appl. Catal. A, Gen. **372**(1), 8–15 (2010)

Karna, M., Lahtinen, M., Valkonen, J.: Preparation and characterization of new low melting ammonium-based ionic liquids with ether functionality. J. Mol. Struct. **922**(1–3), 64–76 (2009)

Kim, K.M., Park, N.G., Ryu, K.S., Chang, S.H.: Characterization of poly(vinylidenefluoride-co-hexafluoropropylene)-based polymer electrolyte filled with $TiO_2$ nanoparticles. Polymer **43**(14), 3951–3957 (2002)

Kohler, F., Roth, D., Kuhlmann, E., Wasserscheid, P., Haumann, M.: Continuous gas-phase desulfurisation using supported ionic liquid phase (SILP) materials. Green Chem. **12**(6), 979–984 (2010)

Mehnert, C.P.: Supported ionic liquid phases. Chemistry **11**(1), 50–56 (2005)

Muldoon, M.J.: Modern multiphase catalysis: new developments in the separation of homogeneous catalysts. Dalton Trans. **39**(2), 337–348 (2010)

Palomar, J., Lemus, J., Gilarranz, M.A., Rodriguez, J.J.: Adsorption of ionic liquids from aqueous effluents by activated carbon. Carbon **47**(7), 1846–1856 (2009)

Riisager, A., Wasserscheid, P., van Hal, R., Fehrmann, R.: Continuous fixed-bed gas-phase hydroformylation using supported ionic liquid-phase (SILP) Rh catalysts. J. Catal. **219**(2), 452–455 (2003)

Riisager, A., Fehrmann, R., Flicker, S., van Hal, R., Haumann, M., Wasserscheid, P.: Very stable and highly regioselective supported

ionic-liquid-phase (SILP) catalysis: continuous flow fixed-bed hydroformylation of propene. Angew. Chem., Int. Ed. Engl. **44**(5), 815–819 (2005a)

Riisager, A., Fehrmann, R., Haumann, M., Gorle, B.S.K., Wasserscheid, P.: Stability and kinetic studies of supported ionic liquid phase catalysts for hydroformylation of propene. Ind. Eng. Chem. Res. **44**(26), 9853–9859 (2005b)

Riisager, A., Fehrmann, R., Haumann, M., Wasserscheid, P.: Supported ionic liquids: versatile reaction and separation media. Top. Catal. **40**(1–4), 91–102 (2006a)

Riisager, A., Fehrmann, R., Haumann, M., Wasserscheid, P.: Supported ionic liquid phase (SILP) catalysis: an innovative concept for homogeneous catalysis in continuous fixed-bed reactors. Eur. J. Inorg. Chem. **4**, 695–706 (2006b)

Rogers, R.D., Seddon, K.R.: Ionic Liquids as Green Solvents: Progress and Prospects, p. 669. American Chemical Society, Washington (2003)

Rogers, R.D., Seddon, K.R.: Ionic Liquids, IIIA: Fundamentals, Progress, Challenges and Opportunities—Transformations and Processes, p. 674. American Chemical Society, Washington (2005)

Ruta, M., Laurenczy, G., Dyson, P.J., Kiwi-Minsker, L.: Pd nanoparticles in a supported ionic liquid phase: highly stable catalysts for selective acetylene hydrogenation under continuous-flow conditions. J. Phys. Chem. C **112**(46), 17814–17819 (2008)

Shi, F., Deng, Y.: Abnormal FT-IR and FTRaman spectra of ionic liquids confined in nano-porous silica gel. Spectrochim. Acta, Part A, Mol. Biomol. Spectrosc. **62**(1–3), 239–244 (2005)

Sun, A.J., Zhang, J.L., Li, C.X., Meng, H.: Gas phase conversion of carbon tetrachloride to alkyl chlorides catalyzed by supported ionic liquids. Chin. J. Chem. **27**(9), 1741–1748 (2009)

van Grieken, R., Serrano, D.P., Aguado, J., Garcia, R., Rojo, C.: Thermal and catalytic cracking of polyethylene under mild conditions. J. Anal. Appl. Pyrolysis **58**, 127–142 (2001)

Vangeli, O.C., Romanos, G.E., Beltsios, K.G., Fokas, D., Kouvelos, E.P., Stefanopoulos, K.L., et al.: Grafting of imidazolium based ionic liquid on the pore surface of nanoporous materials-study of physicochemical and thermodynamic properties. J. Phys. Chem. B **114**(19), 6480–6491 (2010)

Vioux, A., Viau, L., Volland, S., Le Bideau, J.: Use of ionic liquids in sol–gel: ionogels and applications. C. R., Chim. **13**(1–2), 242–255 (2010)

Virtanen, P., Karhu, H., Kordas, K., Mikkola, J.: The effect of ionic liquid in supported ionic liquid catalysts (SILCA) in the hydrogenation of $\alpha, \beta$-unsaturated aldehydes. Chem. Eng. Sci. **62**(14), 3660–3671 (2007)

Virtanen, P., Mikkola, J.P., Toukoniitty, E., Karhu, H., Kordas, K., Eranen, K., et al.: Supported ionic liquid catalysts-from batch to continuous operation in preparation of fine chemicals. Catal. Today **147**, S144 (2009a)

Virtanen, P., Karhu, H., Toth, G., Kordas, K., Mikkola, J.P.: Towards one-pot synthesis of menthols from citral: modifying supported ionic liquid catalysts (SILCAs) with Lewis and Bronsted acids. J. Catal. **263**(2), 209–219 (2009b)

Wasserscheid, P., Welton, T.: Ionic Liquids in Synthesis. Wiley–VCH, Weinheim (2008)

Welton, T.: Room-temperature ionic liquids. Solvents for synthesis and catalysis. Chem. Rev. **99**, 2071 (1999)

Werner, S., Szesni, N., Bittermann, A., Schneider, M.J., Harter, P., Haumann, M., et al.: Screening of supported ionic liquid phase (SILP) catalysts for the very low temperature water-gas-shift reaction. Appl. Catal. A, Gen. **377**(1–2), 70–75 (2010)

Wu, W.Z., Han, B.X., Gao, H.X., Liu, Z.M., Jiang, T., Huang, J.: Desulfurization of flue gas: $SO_2$ absorption by an ionic liquid. Angew. Chem., Int. Ed. Engl. **43**(18), 2415–2417 (2004)

Zhang, Z.M., Wu, L.B., Dong, J., Li, B.G., Zhu, S.P.: Preparation and $SO_2$ sorption/desorption behavior of an ionic liquid supported on porous silica particles. Ind. Eng. Chem. Res. **48**(4), 2142–2148 (2009a)

Zhang, J., Ma, Y., Shi, F., Liu, L., Deng, Y.: Room temperature ionic liquids as templates in the synthesis of mesoporous silica via a sol–gel method. Microporous Mesoporous Mater. **119**(1–3), 97–103 (2009b)